ADVANCED HEALTHCARE MATERIALS

Supporting Information

for *Adv. Healthcare Mater.*, DOI 10.1002/adhm.202303267

Genetically Engineered Macrophages Co-Loaded with CD47 Inhibitors Synergistically Reconstruct Efferocytosis and Improve Cardiac Remodeling Post Myocardial Ischemia Reperfusion Injury

Haipeng Tan, Weiyan Li, Zhiqing Pang, Xueyi Weng, Jinfeng Gao, Jing Chen, Qiaozi Wang, Qiyu Li, Hongbo Yang, Zheng Dong, Zhengmin Wang, Guangrui Zhu, Yiwen Tan, Yuyuan Fu, Chengzhi Han, Shiteng Cai, Juying Qian, Zheyong Huang, Yanan Song* and Junbo Ge**

Genetically Engineered Macrophages Co-loaded with CD47 Inhibitors Synergistically Reconstruct Efferocytosis and Improve Cardiac Remodeling Post Myocardial Ischemia Reperfusion Injury

Haipeng Tan, Weiyan Li, Zhiqing Pang, Xueyi Weng, Jinfeng Gao, Jing Chen, Qiaozi Wang, Qiyu Li, Hongbo Yang, Zheng Dong, Zhengmin Wang, Guangrui Zhu, Yiwen Tan, Yuyuan Fu, Chengzhi Han, Shiteng Cai, Juying Qian, Zheyong Huang, Yanan Song*, Junbo Ge**

Contents:

Figure S10. Synthesis and characterization of DSPE-PEG2k-TK-PEP-20.

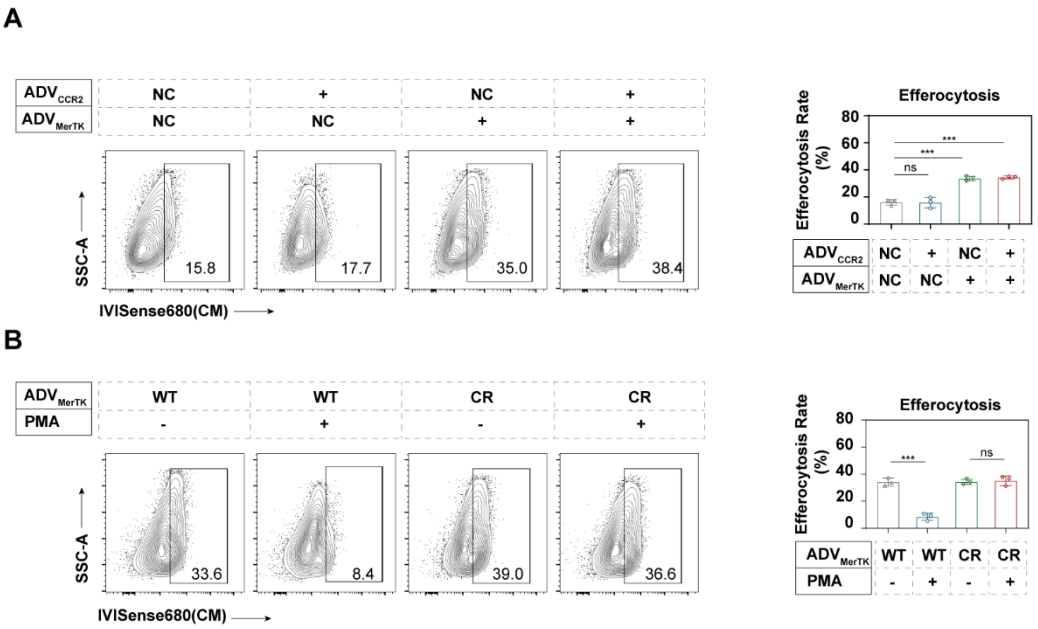

Figure S1. Flow cytometry validation of macrophage efferocytosis capacity after genetic engineering modification. (A) The impact of CCR2 and MerTK overexpression on macrophage efferocytosis (*n*=3). The impact of MerTK cleavage-resistant mutation on macrophage efferocytosis under stimulation of PMA, an ADAM17 agonist (*n*=3). Results are presented as mean ± SD, ^{ns}P > 0.05, *P < 0.05, *P < 0.01, *P < 0.001.

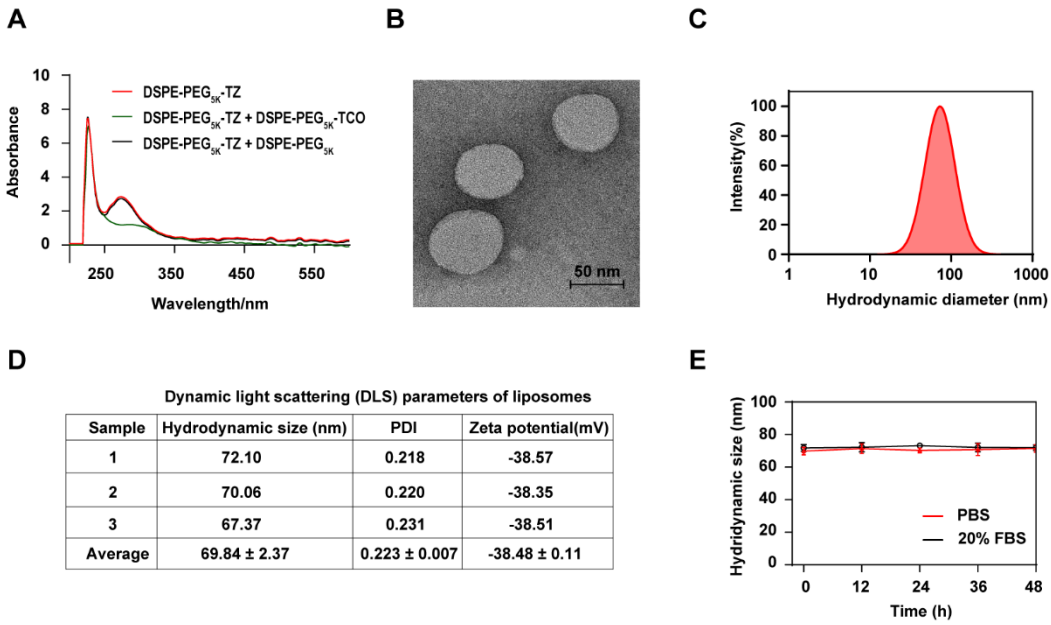

Dynamic light scattering (DLS) parameters of liposomes

Sample	Hydrodynamic size (nm)	PDI	Zeta potential(mV)
1	72.10	0.218	-38.57
2	70.06	0.220	-38.35
3	67.37	0.231	-38.51
Average	69.84 ± 2.37	0.223 ± 0.007	-38.48 ± 0.11

Figure S2. Characterization of click reaction and liposomes loaded PEP-20. (A) The UV spectral profile of DSPE-PEG5k-TZ before and after incubation with DSPE-PEG5k-TCO or DSPE-PEG5k for 10 min (n = 3). (B) Representative transmission electron microscopy image of liposomes. Scale bar, 50 nm. (C) and (D) Hydrodynamic size, polymer dispersity index (PDI) and zeta potential of liposomes measured by dynamic light scattering (*n*=3). (E) The hydrodynamic size of liposomes measured by dynamic light scattering after incubation at PBS and 20% FBS at different time points (*n*=3).

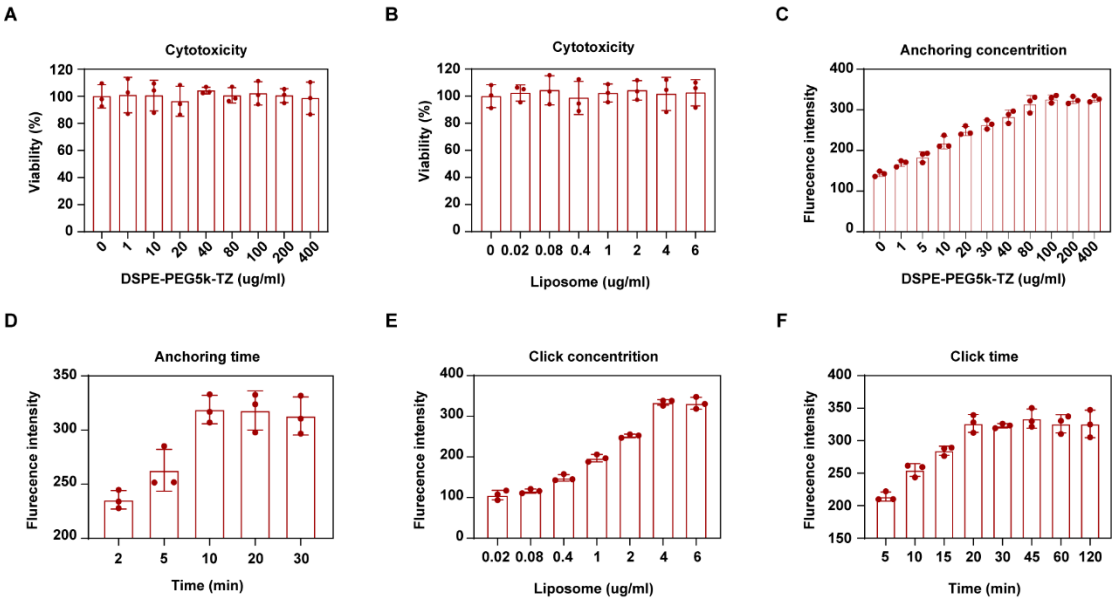

Figure S3. In vitro cytotoxicity and optimization of anchoring and clicking concentration and time. (A) In vitro cytotoxicity of different concentrations of DSPE-PEG5k-TZ on macrophages for 24 h (*n*=3). (B) In vitro cytotoxicity of different concentrations of liposomes on macrophages for 24 h (*n*=3). (C)The optimization of liposome-coupling efficiency at different concentrations of cell membrane anchoring module (DSPE-PEG5k-TZ) when the concentration of liposomes, anchoring time and click time were set as 6 mg mL^{-1}, 20 min and 30 min, respectively (*n*=3). (D) The optimization of liposome-coupling efficiency at different incubation times with 80 μg mL^{-1} DSPE-PEG5k-TZ, while the concentration of liposomes and click time were set as 6 mg mL^{-1} and 30 min, respectively (*n*=3). (E) The optimization of liposome-coupling efficiency at different concentrations of liposomes, when the concentration of DSPE-PEG5k-Tre, anchoring time and click time were set as 80 ug mL^{-1}, 10 min and 30 min, respectively (*n*=3). (F) The optimization of liposome-coupling efficiency at different click times, when the

concentration of DSPE-PEG5k-Tre, anchoring time and concentration of liposomes were set as 80 ug mL^{-1}, 10 min and mg mL^{-1}, respectively (*n*=3).

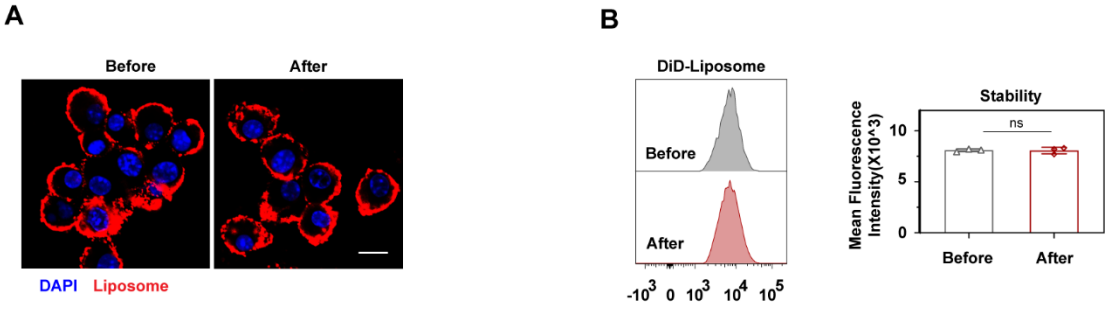

Figure S4. Anchoring stability after freeze-thaw cycle. (A) the anchoring of liposomes on the surface of macrophages was visualized under confocal microscope before and after -80 ℃ freezing. Scale bar, 10 μm. (B) the anchoring of liposomes on the surface of macrophages was quantified by flow cytometry before and after -80 ℃ freezing(n=3). Results are presented as mean ± SD, $^{ns}P > 0.05$, *P < 0.05, *P < 0.01, *P < 0.001.

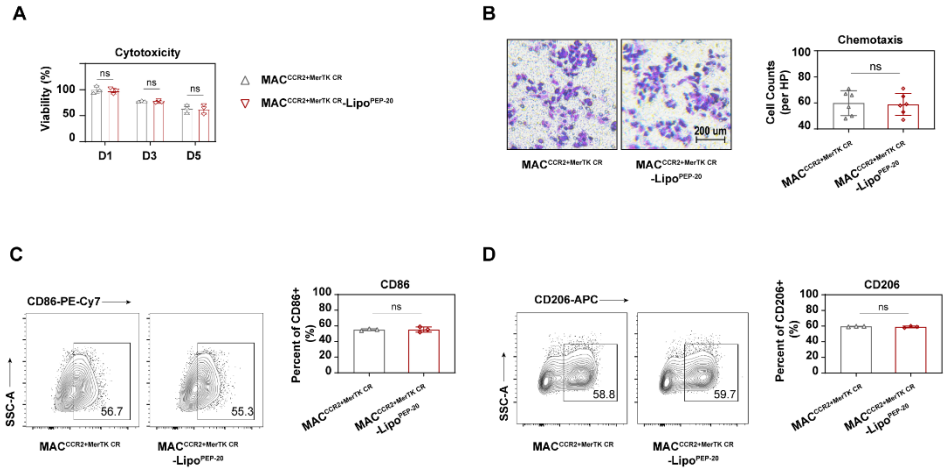

Figure S5. Evaluation of the impact of liposome coupling on the physiological functions of engineered macrophages. (A) In vitro cytotoxicity of liposome

coupling on macrophages for 1 d, 3d and 5d (*n*=3). (B) Transwell assay of engineered macrophages towards 20 ng ml^{-1} MCP-1 before and after liposome anchoring (*n*=3). (C) and (D) Flow cytometry assay of macrophage polarization state before and after liposome anchoring (*n*=3). Results are presented as mean ± SD, $^{ns}P > 0.05$, $*P < 0.05$, $*P < 0.01$, $*P < 0.001$.

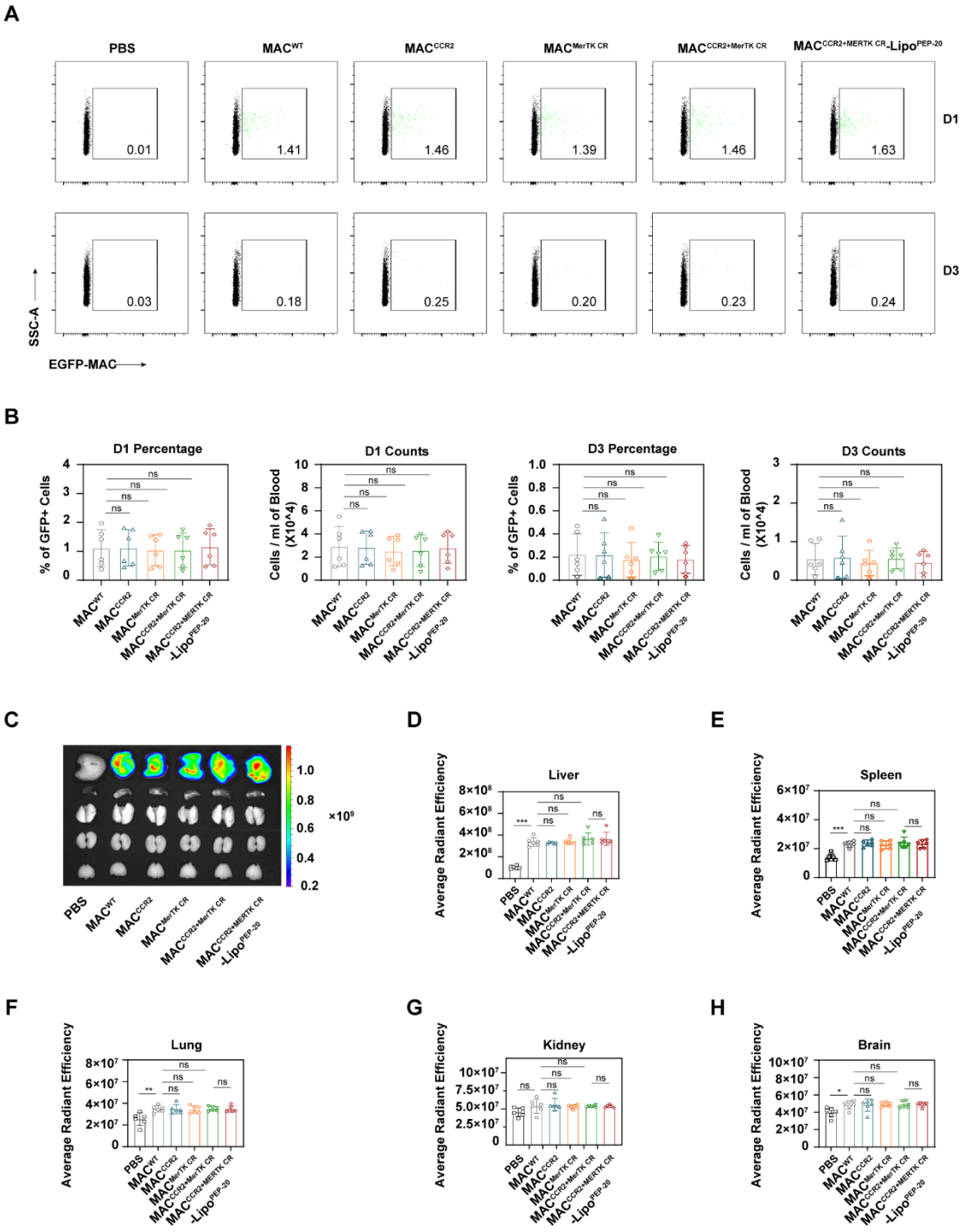

Figure S6. Biodistribution of MAC$^{CCR2+MerTK\ CR}$-Lipo^{PEP-20} in vivo. (A) The retention of MAC$^{CCR2+MerTK\ CR}$-Lipo^{PEP-20} and various control groups in the mice bloodstream at 1 day and 3 days after intravenous injection were detected by flow cytometry, and was quantified in (B) (*n*=6). (C) IVIS images of major organs of MI/R induced mice after treated with each group IVISense 680 labeled macrophages, and

were quantified in (D) liver, (E) spleen, (F) lung, (G) kidney and (H) brain (*n*=6). Results are presented as mean ± SD, $^{ns}P > 0.05$, *P < 0.05, *P < 0.01, *P < 0.001.

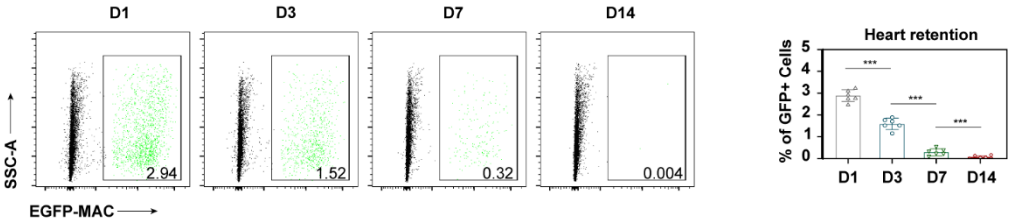

Figure S7. The retention of adaptive MAC$^{CCR2+MerTK\ CR}$-Lipo^{PEP-20} in the injured heart. The percentage of adaptive GFP+ MAC$^{CCR2+MerTK\ CR}$-Lipo^{PEP-20} in all non-myocardium of the injured heart was measured by flow cytometry at D1, D3, D7 and D14 post administration(n=6). Results are presented as mean ± SD, $^{ns}P > 0.05$, *P < 0.05, *P < 0.01, *P < 0.001.

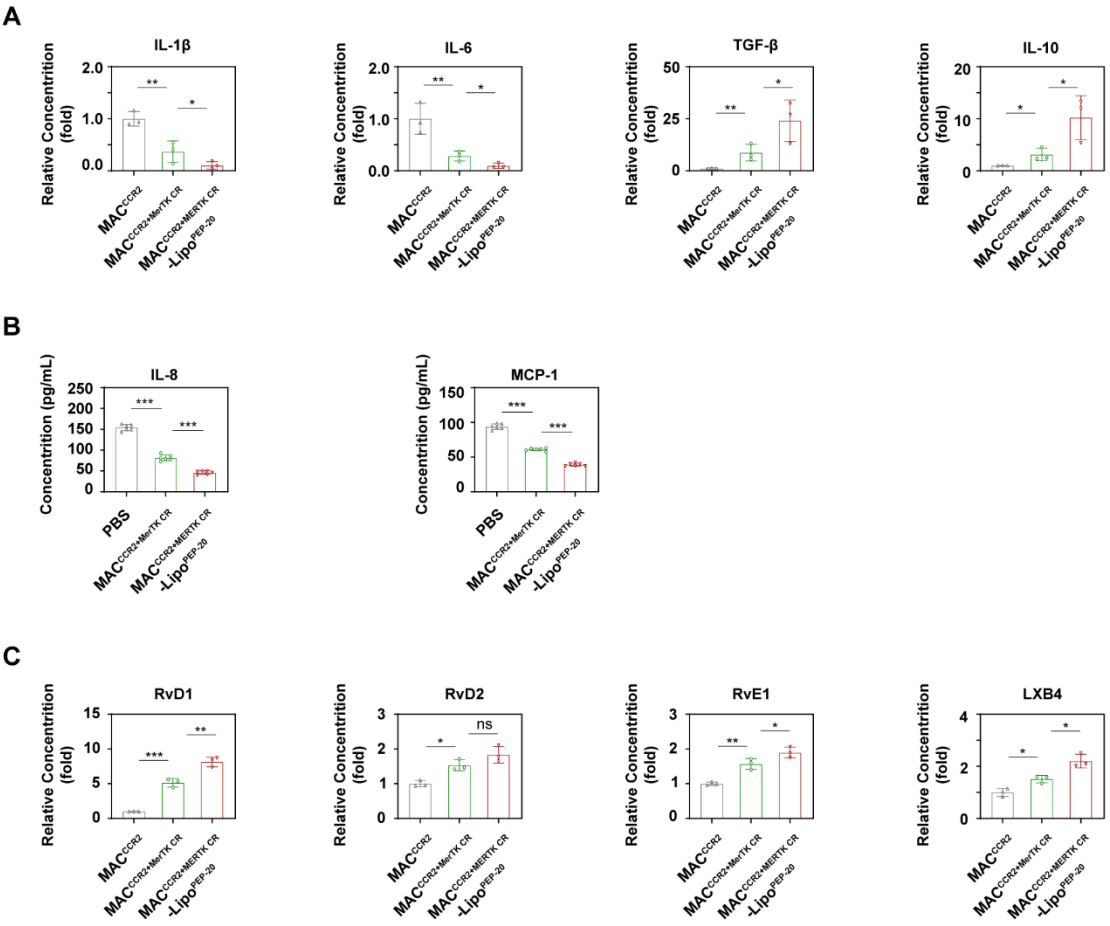

Figure S8. The influence of efferocytosis optimization on macrophages. (A) Real-time quantitative reverse transcription polymerase chain reaction (RT-qPCR) detection of cytokines(IL-1 β , IL-6, TGF- β , IL-10) of MAC^{CCR2}, $MAC^{CCR2+MerTK\ CR}$ or $MAC^{CCR2+MerTK\ CR}$-$Lipo^{PEP-20}$ after apoptotic cardiomyocyte feeding(n=3). (B) The concentration of two typical chemokines (IL-8 and MCP-1) were quantified by ELISA assay in PBS, $MAC^{CCR2+MerTK\ CR}$ or $MAC^{CCR2+MerTK\ CR}$-$Lipo^{PEP-20}$ treated MI/R mice serum (n=6). (C) ELISA analysis of SPMs (RvD1, RvD2, RvE1 and LXA4) concentrations in culture medium of MAC^{CCR2}, $MAC^{CCR2+MerTK\ CR}$ or $MAC^{CCR2+MerTK\ CR}$-$Lipo^{PEP-20}$ after apoptotic cardiomyocyte feeding(n=3). Results are presented as mean ± SD, $^{ns}P > 0.05$, *P < 0.05, *P < 0.01, *P < 0.001.

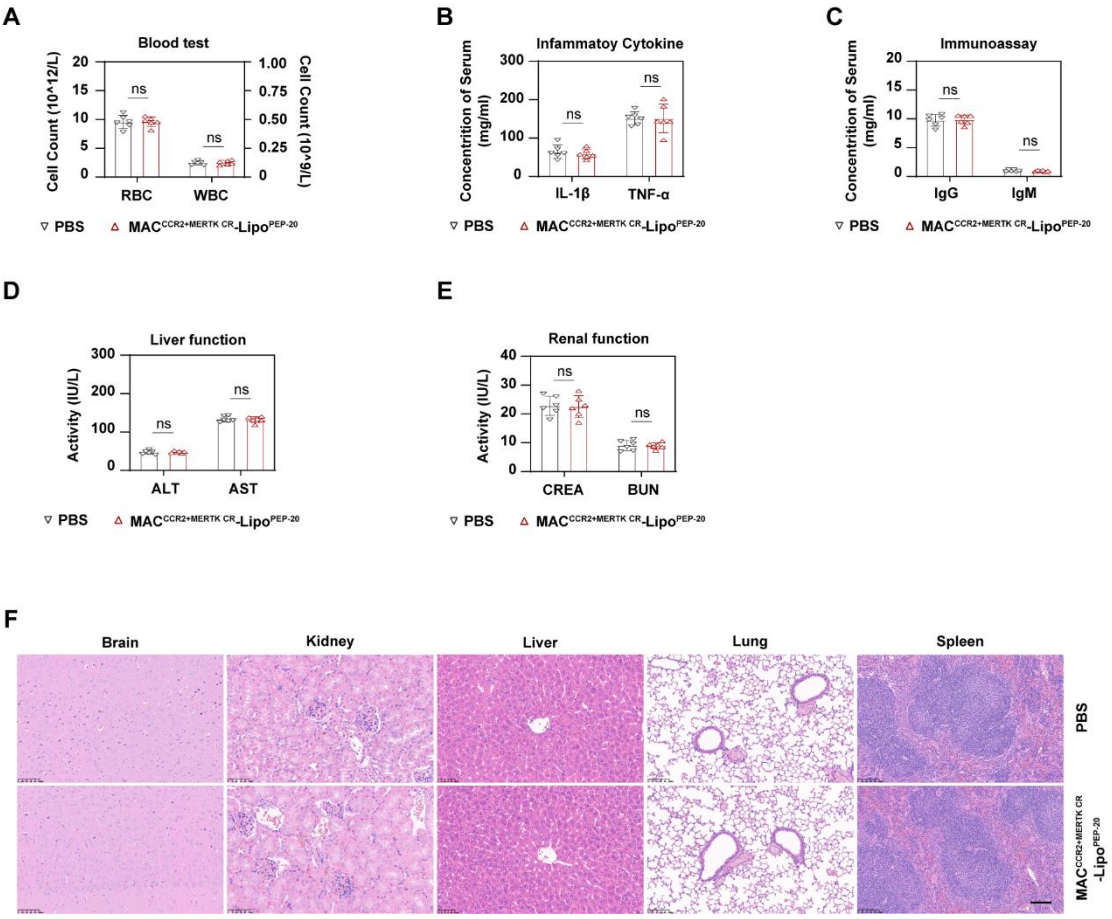

Figure S9. Biosafety of MAC$^{CCR2+MerTK\ CR}$-Lipo^{PEP-20} in vivo. (A) Blood routine examination of healthy mice 1 day after treatment with PBS or MAC$^{CCR2+MerTK\ CR}$-Lipo^{PEP-20} (*n*=6). (B) Serum concentration of inflammatory cytokines (IL-1β, TNF-α) of healthy mice detected by ELISA at 3 d post administration of PBS or MAC$^{CCR2+MerTK\ CR}$-Lipo^{PEP-20} (*n*=6). (C) ELISA assay of immune response indicated by serum level of general IgG and IgM of healthy mice with or without MAC$^{CCR2+MerTK\ CR}$-Lipo^{PEP-20} treatment (*n*=6). Biochemical test of (D) liver and (E) renal function of healthy mice after PBS or MAC$^{CCR2+MerTK\ CR}$-Lipo^{PEP-20} administered (*n*=6). (F) Histology characteristics of major organs of PBS or MAC$^{CCR2+MerTK\ CR}$-

Lipo^{PEP-20} treated healthy mice were evaluated by HE staining (n=6). Scale bar 100 um. Results are presented as mean ± SD, ^{ns}P > 0.05, *P < 0.05, *P < 0.01, *P < 0.001.

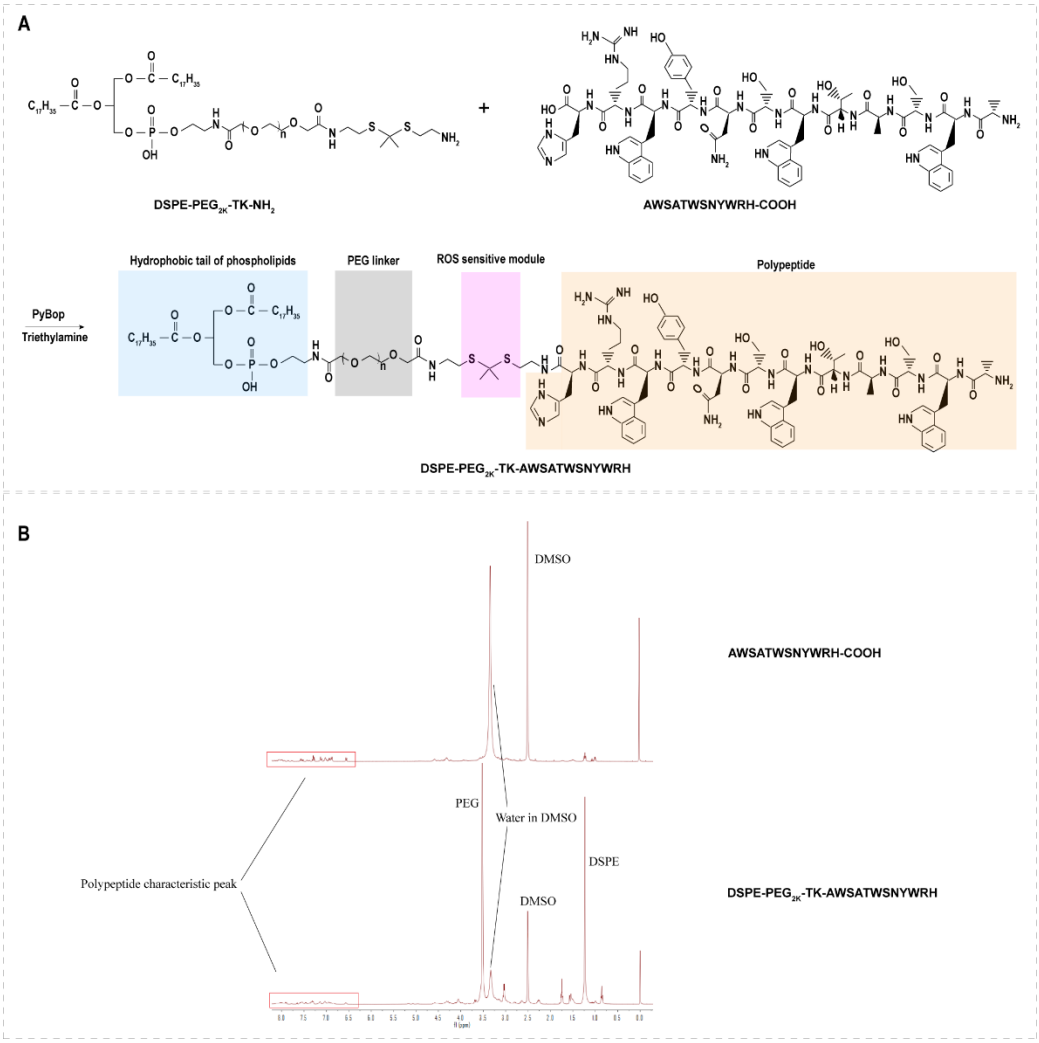

Figure S10. Synthesis and characterization of DSPE-PEG2k-TK-PEP-20. (A) The synthesis and structure of DSPE-PEG2k-TK-PEP-20. (B) The structure of DSPE-PEG2k-TK-PEP-20 was verified by ^{1}H-NMR.